# THE NATURE OF OPERATING FLIGHT LOADS AND
# THEIR EFFECT ON PROPULSION SYSTEM STRUCTURES

Kenneth H. Dickenson
Richard L. Martin
Boeing Commercial Airplane Company

## ABSTRACT

Past diagnostics studies revealed the primary causes of performance deterioration of high by-pass turbofan engines to be flight loads, erosion and thermal distortion. This paper examines the various types of airplane loads that are imposed on the engine throughout the lifetime of an airplane. These include flight loads from gusts and maneuvers and ground loads from take-off, landing and taxi conditions. Clarification is made in definitions of the airframer's limit and ultimate design loads and the engine manufacturer's operating design loads. Finally, the influence of these loads on the propulsion system structures is discussed.

## INTRODUCTION

The traditional transport airplane structures analyst's treatment of an engine is very simple: The engine is a "concrete block" whose properties are entirely inertial, and the main concerns are that it should not fall off the strut and that it is located properly from a wing flutter viewpoint (figure 1). In the era of the turbojet and the low bypass ratio turbofan, such treatment was acceptable because it was nearly correct. Engines and their inlets were so compact and rigid (figure 2) that the internal structural problems could be left to the engine manufacturers who needed only to be advised of the accelerations to be applied at the mount locations.

In the late 1960's the advent of the high bypass ratio turbofan engine with it's large fan case relative to its core brought change. Early in the Boeing 747 program, for example, it was found that thrust forces caused "ovalization" of the engine case because the engine's combination of large diameter (figure 3) and high thrust imposed a substantial couple at the engine mounts. This problem was alleviated by adding a "thrust yoke" that transferred thrust directly to the strut and reduced distortion of the case due to thrust.

The high bypass ratio turbofan engines have large inlet airflows relative to the engine core size. Thus, a large momentum change is required to align the airflow with the engine at high angles of attack. Since inlets are usually bolted to the front flange of the fan case, the inlet aerodynamic loads associated with this momentum change induce bending and distortion into the smaller diameter engine core case. These case distortions may cause rubbing between the rotors and the static case structure while the desire for higher overall pressure ratio requires better control of tip clearances. The aerodynamically induced operating loads

that act on the inlet are modest in comparison to overall airframe design loads. It remained for the 1973 oil embargo and the ensuing dramatic rise in fuel prices to motivate a deeper investigation of airframe and engine structural interaction.

Attention was focused on the causes of engine fuel consumption deterioration in the NASA sponsored Pratt & Whitney Aircraft JT9D Diagnostics Program. In this effort, several different probable deterioration mechanisms were identified and evaluated analytically. Prominent among them was rubbing between the rotor tips (of the fan, compressors, and turbines) and the engine case caused by flexing of the engine under operating loads. The result of rubbing was increased clearance between the rotor and case since material was worn from the "rub strips" and the blade tips. Increased clearance reduced component efficiency and increased specific fuel consumption.

## AIRPLANE LOADS

### Design Loads

Due to the overriding importance of safety, airplane design loads have been studied intensively for many years and are the subject of a large body of doctrine and practice developed by airframe manufacturers and enforced by the Federal Aviation Administration (FAA). A "limit design load" is determined for airframe structure as the maximum load that the structure can be expected to encounter during the entire life of the airplane fleet. At the limit design load, the structure is not permitted to suffer permanent deformation; i.e., the maximum stress may not exceed the elastic limit. To provide an added degree of safety, an "ultimate design load" is also specified, usually as 1.5 times the limit load value. Up to the ultimate load, the structure is permitted to suffer "permanent set", but it must not fail.

The design loads are determined by analyzing the airplane in a variety of load conditions that are contained within the envelope of the "V - n diagram" (a plot of the accelerations that the airplane must withstand versus airspeed). Three main types of load conditions are considered. The first is maneuver. Transport category airplane limit loads are determined in 2.5 g turns or pull-ups with flaps retracted and in 2.0 g turns with flaps down. The second type of load condition is due to atmospheric turbulence. It is assumed that gusts of a defined shape and velocity will be encountered by the airplane at speeds specified in relation to the design operating speed limits chosen by the manufacturer. The airplane's response is determined by analyzing the aerodynamic, elastic, and inertial characteristics in detail. The third loading category is associated with the ground. These loading conditions include take-off, landing and taxi. Analytically determined design loads are corroborated by extensive flight load surveys using accelerometers, strain gages and pressure transducers.

The oustanding structural safety records of today's commercial air fleets demonstrate that the design loads issues are very well understood. However, the loads that cause day-to-day TSFC deterioration are less severe than design loads

and are not so well understood. They may be termed "operating" loads, and a different approach is needed to understand them.

## Operating Loads

The parameters for determining operating loads are the same as those for design loads; i.e., airplane aerodynamic, elastic, and inertial properties on the one hand, and flight conditions (maneuvers, turbulence, etc.) on the other. To a considerable degree, the problem resembles that of analyzing structural fatigue. Service life, maintenance, and economy are the main considerations, with statistical descriptions of the operating environment being the scenario, as opposed to a set of extreme conditions.

Fatigue damage is assessed from the cumulative occurences of different stress levels. The part of TSFC degradation due to clearance change, on the other hand, depends on the probable time period (or number of flights) until any given load level is exceeded once. Figure 4 shows the analysis sequence. The starting point is the set of mission profiles that typify the airplane's utilization (upper left corner). Mission length is important because it determines how many "ground-air-ground" (GAG) cycles are flown per hour of operation. The altitude and speed profiles determine the frequency and severity of gusts.

Load exceedance probability per flight can be inferred from airplane characteristics and the mission profile. The sketch at the upper right of figure 4 refers to inertia load exceedances, but a similar plot can relate to airloads. When the probable loads are known, the probable tip clearance changes can be inferred from the elastic properties of the engine itself. These may be obtained by analyses varying from simple beam representations to finite-element models containing thousands of elements. Recent experience supports the need for the more complex finite-element approach. When tip clearances become negative, rubs are indicated, and TSFC deterioration can be expected.

In addition to revenue service missions, other flight profiles must be considered, such as crew training. A significant mission that occurs only once on each airplane is the "acceptance flight" (figure 5). All transport airplanes are checked for satisfactory flight characteristics and functioning of warning systems before delivery to the customer airline. In such flights, the airplane is not tested to the limit loads of the flight design envelope but to more normal operating conditions, such as maximum airspeed (dynamic pressure), maximum Mach number, and minimum airspeed (stall warning) where warning devices such as stick shakers automatically alert the pilot to the situation. Since such a flight always occurs first in an airplane's history, it establishes a starting set of rubs and clearances for subsequent exceedance studies.

Statistical descriptions of the inertia load environment have been obtained by accumulation of a great many speed/acceleration/altitude ("VGH") recordings made in actual airline service (figure 6). Airspeed (V), normal acceleration (g), and altitude (H) are recorded continuously. The recordings are later analyzed by

counting acceleration peaks. The number of "occurrences" of a particular acceleration level is defined as the number of peaks found over some time period that fall between the upper and lower bounds of that level. The number of "exceedances" of that level is the sum of the occurrences of that level and all higher levels as shown in figure 7.

Histograms (figure 8) can then be constructed which show occurrences and exceedances per flight hour or per flight versus load level, and plots such as shown in figure 9, depicting probable nacelle inertia load exceedances, can be drawn. This figure, incidentally, shows a characteristic feature of the environment of wing-mounted engines. The motions and accelerations of the nacelles are larger than those at the airplane center of gravity because of the wing aeroelastic response to dynamic loads such as gusts and landing impacts. In additon to accelerations, gyroscopic loads caused by airplane angular motions must also be considered.

Under normal conditions, the most severe engine aerodynamic loading occurs at takeoff when the maximum engine thrust produces a high mass flow rate through the inlet combined with a high angle of attack. These effects are illustrated in figure 10 which shows low pressure caused by suction on the lower inside lip of the inlet. This is associated with high local velocity as the flow turns sharply. Supersonic flow usually occurs in this region, followed by shocks and sometimes by local flow separation.

Of lesser importance, but significant because it is a condition that creates a load reversal, is the maximum dynamic pressure condition shown in figure 11. This condition involves a negative local inlet angle of attack and an inlet pitching moment acting downward. This moment is, however, of much smaller magnitude than the nose-up moment at takeoff.

Neither the maximum dynamic pressure condition nor the one shown in figure 12 -- stall warning at $10^{o}$ flaps -- are normal revenue service flight conditions. Both of these, however, are currently flown in the flight acceptance test of every new airplane.

One of the more uncertain assumptions regarding inlet pressures has been the circumferential distribution. A simple, one wave cosine distribution, illustrated in figure 13, rotated to account for non-symmetric effects has been customary. This assumption awaits validation by the results of the Nacelle Aerodynamic and Inertia Loads (NAIL) flight test program.

To illustrate the joint efforts in the JT9D Diagnostics Program and the interdependence of the engine and airframe manufacturer in the propulsion interface, Figure 14 shows the mathematical model used to analyze the 747 propulsion system. Government and industry foresight several years ago provided the NASTRAN finite element program giving wide availability to this technology. Air breathing propulsion structures are a relatively late application of this technology, and there is currently a large effort being made toward test and analysis correlations to enhance this application.

Currently, Boeing and the three major jet engine manufacturers are utilizing the type of models illustrated here to calculate deflections, clearance changes, internal loads, and vibration behavior on the 767, 757 and 737-300 new airplane programs and on future powerplant installations for the 747 airplane program.

The airframe and engine manufacturer must each conduct their own analyses for their specific needs. An exchange of data files provides each with this capability and the integrated model as illustrated in figure 15. Recent trends in nacelle design have resulted in much closer structural coupling between the engine, nacelle, and strut. For example, in the 767 design the front mounting system has been placed to minimize thrust bending moment, and the thrust reverser and fan exhaust cowling are hinged from the strut and clamp onto the engine through circumferential V-grooves. This not only simplifies engine removal and maintenance but also serves as a dual load path with the mounts which provides the redundancy required for fail safe design in case of mount failure. An extra benefit from this dual load path is a reduction of engine loading which enhances engine performance through reduced clearance changes under flight operating loads. The close coupling inherent in this type of design necessitates use of detailed nacelle-engine-strut finite element models to define interface loads accurately.

A characteristic of engine structure relative to conventional airframe structure is its inherently greater stiffness and complexity. This obviously must be the case in order to maintain the dimensional constraints so important to engine performance. The maximum engine bending deformations are typically one to two orders of magnitude less than maximum strut deflection as exhibited in figure 16 for a "g" loading condition. The attainment of accuracy in the engine and nacelle math model comparable to conventional airframe structures , therefore, requires a great deal of experience and effort and should rely heavily on accurately measured data when available.

To illustrate this point, figure 17 shows typical calculated clearance change contour lines for a normal takeoff condition. This plot is for the inboard side of the number three engine on the 747 airplane. Clearance closure is denoted by the shaded regions. The information shown here is used by the engine manufacturer in a separate post processor program that calculates blade rubs, stage-by-stage clearance increases, and TSFC deterioration.

The ultimate goal in the diagnostics effort is to provide adequate data for taking actions toward eliminating performance deterioration. Much of the required data has been generated in the early tasks. The flight loads portion of the JT9D Diagnostics Program in which engine clearance changes are measured in flight and the concurrent NAIL flight loads program will complete the data. The task ahead is the application of this data and the appropriate use of design tools in concerted efforts between the engine and airframe manufacturers to reduce performance deterioration. A considerable effort has evolved in the area of integrated engine-nacelle design studies aimed at stiffening current power plant installations. More important is the use of the diagnostics data in systems currently under design and development that recognize and build deterioration prevention into the initial designs.

179

# DESIGN LOAD PHILOSOPHY
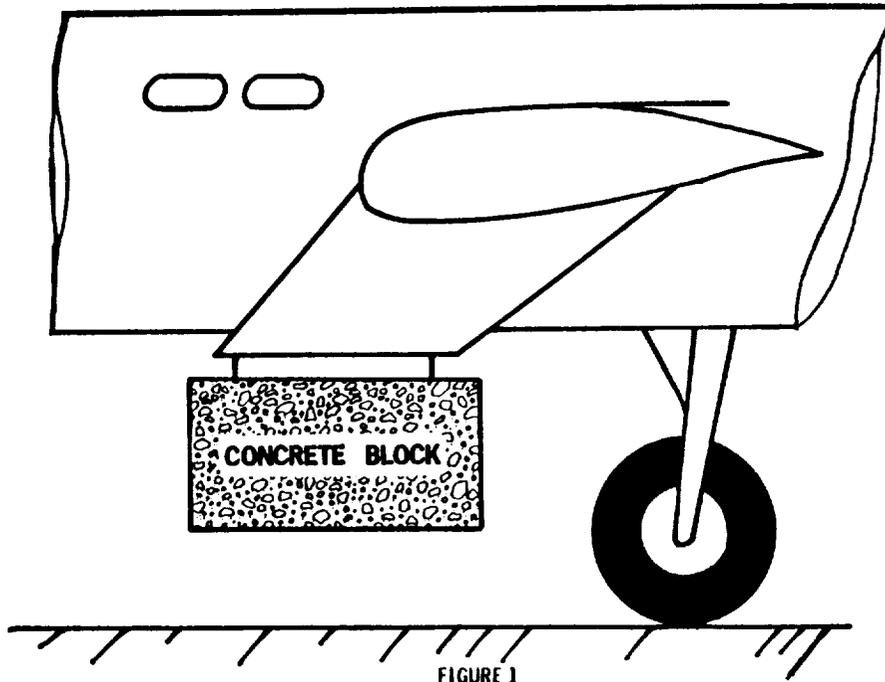


FIGURE 1

# EARLY TURBOJET INSTALLATION
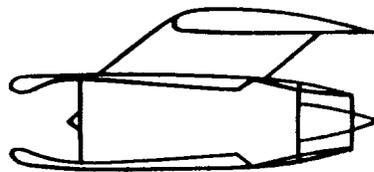


FIGURE 2

# MODERN ENGINE INSTALLATION
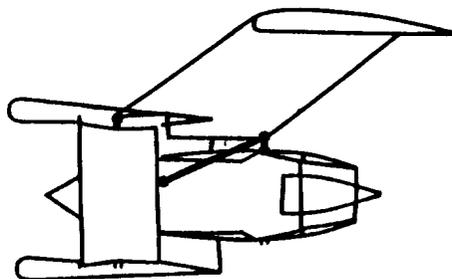


FIGURE 3

# RELATION OF AIRPLANE FLIGHT LOAD EXCEEDANCES TO BLADE TIP CLEARANCE
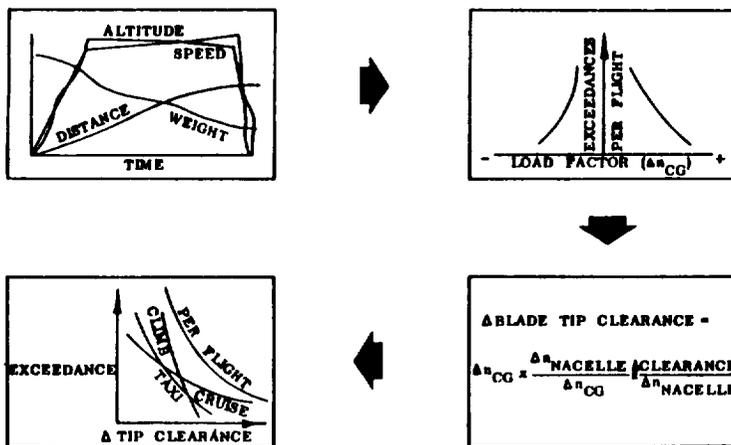


FIGURE 4

## ACCEPTANCE FLIGHT PROFILE

CRUISE

MAXIMUM MACH NO.

SHUTDOWN/RESTART

MAXIMUM DYNAMIC
PRESSURE

ALTITUDE

STALL
WARNING

DESCENT

CLIMB

TOUCH AND GO

TAKEOFF

TIME

LAND, REVERSE
THRUST
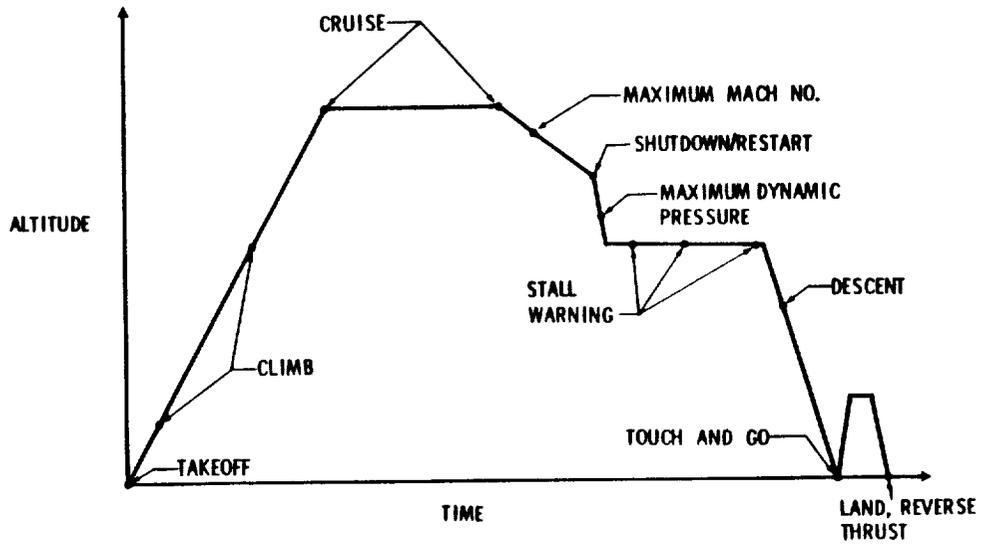
FIGURE 5

## ILLUSTRATIVE VGH RECORDING

FLIGHT PHASE ——→ CLIMB    ENROUTE    DESCENT

ALTITUDE    AIRSPEED

ACCEL

ACCEL.
TYPE ——→ TAXI AND    GUST    MANEUVER    LANDING
TAKE-OFF    IMPACT

FIGURE 6

182
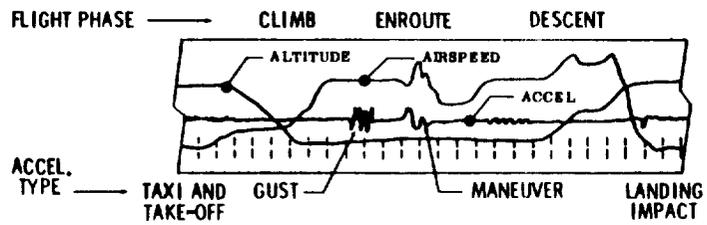
# ANALYSIS OF LOAD FACTOR TIME HISTORY
## FROM VGH RECORDER
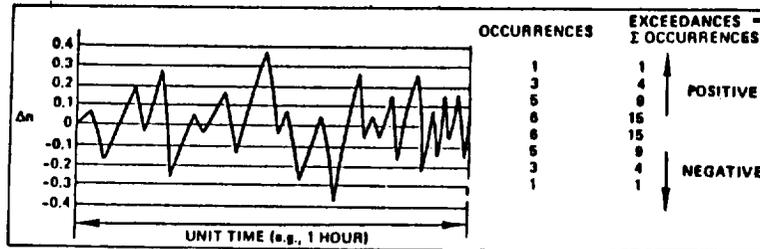


**FIGURE 7**

# HISTOGRAM AND PLOT OF OCCURRANCES



**FIGURE 8**

183
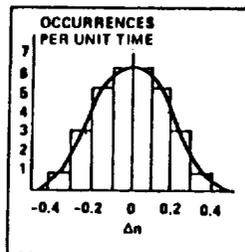
# NACELLE LOAD EXCEEDANCE DATA
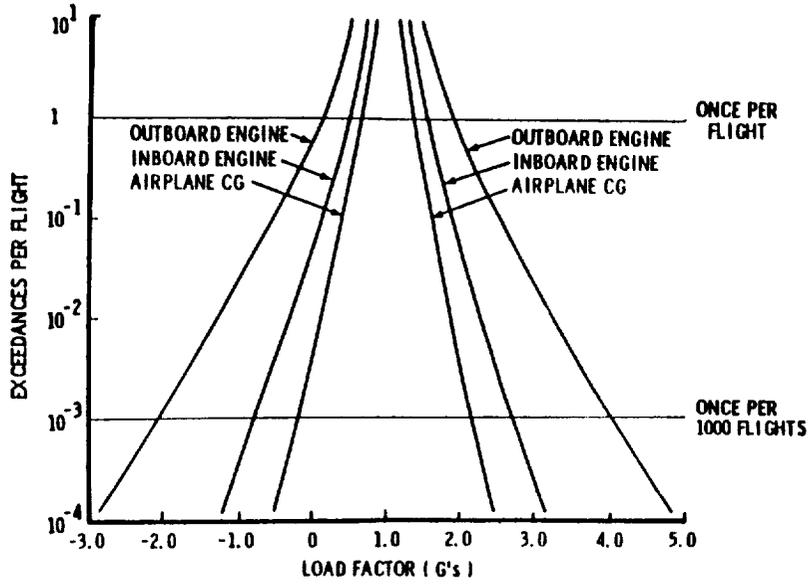


FIGURE 9

# AIRLOADS

TAKEOFF ROTATION



PRESSURE
DISTRIBUTION

RESULTANT
LOADS

FIGURE 10

184
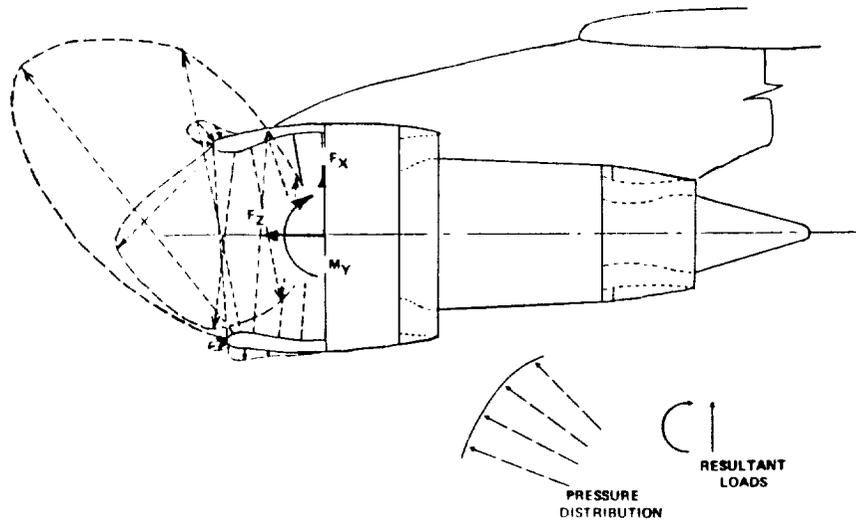
# AIRLOADS

MAXIMUM DYNAMIC PRESSURE
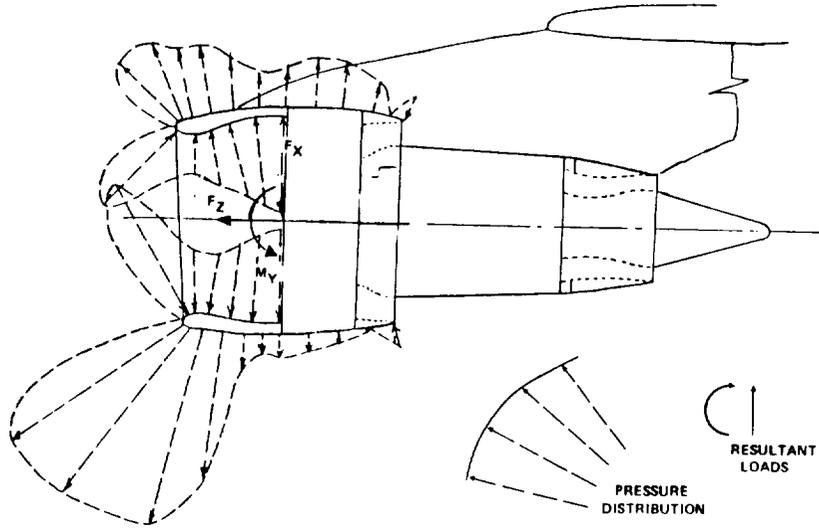


FIGURE 11

# AIRLOADS

STALL WARNING, $10^0$ FLAPS
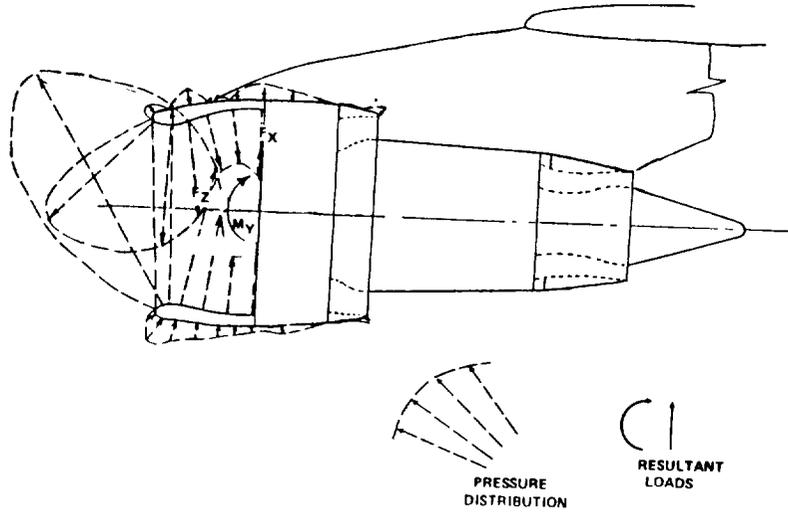


FIGURE 12

# INLET CIRCUMFERENTIAL PRESSURE DISTRIBUTION
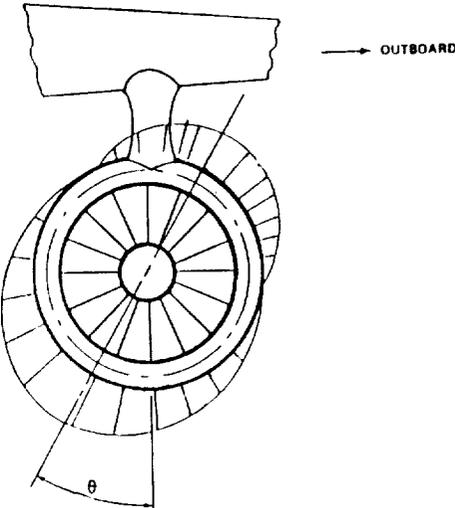


FIGURE 13

# PROPULSION SYSTEM SUBSTRUCTURES AND RESPONSIBILITIES
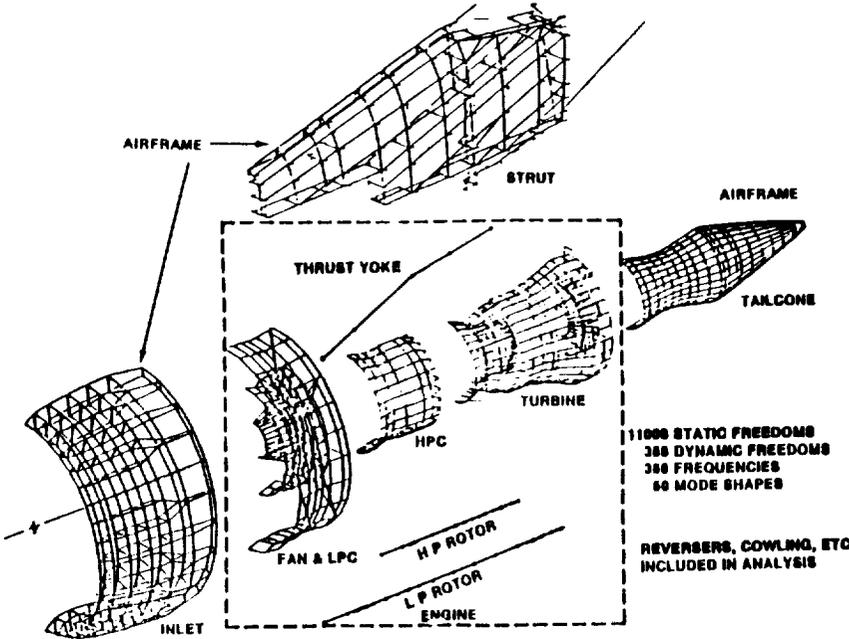


FIGURE 14

# FINITE ELEMENT MODEL

WING BOX
ATTACH POINTS
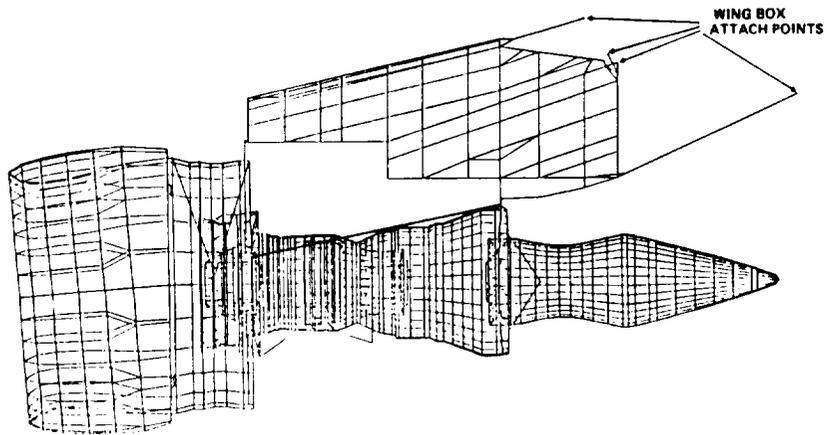
FIGURE 15

# STRUCTURAL DEFLECTION

ORIGINAL

DEFLECTED

FIGURE 16

187
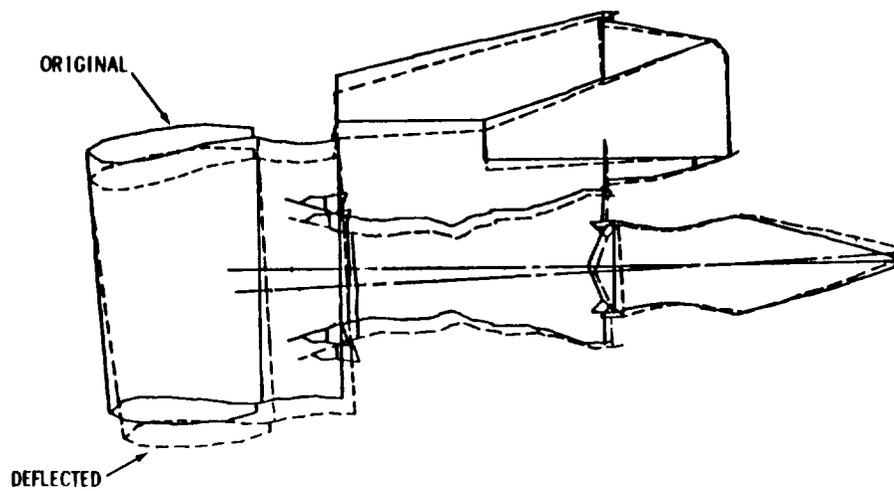
# CALCULATED CLEARANCE CHANGES (INCHES)



FIGURE 17

188